Links between hydrogen bonding, residual stress, structural properties and metastability in hydrogenated nanostructured silicon thin films

2003 J. Phys.: Condens. Matter 15 7185

(http://iopscience.iop.org/0953-8984/15/43/004)

INSTITUTE OF PHYSICS PUBLISHING JOURNAL OF PHYSICS: CONDENSED MATTER

J. Phys.: Condens. Matter **15** (2003) 7185–7200 PII: S0953-8984(03)66319-8

Links between hydrogen bonding, residual stress, structural properties and metastability in hydrogenated nanostructured silicon thin films

S Vignoli[1], R Butté[1,2], R Meaudre[1], M Meaudre[1] and R Brenier[1]

[1] Laboratoire de Physique de la Matière Condensée et des Nanostructures (UMR 5586 CNRS), Université Claude Bernard Lyon 1, F-69622 Villeurbanne Cedex, France
[2] Department of Physics and Astronomy, University of Sheffield, Sheffield S3 7RH, UK

E-mail: svignoli@lpmcn.univ-lyon1.fr

Received 15 July 2003, in final form 18 September 2003
Published 17 October 2003
Online at stacks.iop.org/JPhysCM/15/7185

Abstract

We present a systematic study of the local hydrogen bonding in hydrogenated polymorphous silicon thin films (pm-Si:H), a heterogeneous material deposited on the edge of crystallinity, by means of Fourier transform infrared spectroscopy. A vibrational mode at $\sim$2030 cm^{-1} is reported and attributed to hydrogen atoms bonded in hydrogen-rich regions present at the interface between ordered regions and the amorphous matrix. This assignment is found to be in good agreement with previous spectroscopic ellipsometry and Raman spectroscopy studies. Combined with stress measurements we draw a picture of the nanostructure of pm-Si:H films, namely a two-domain material exhibiting: (i) large fluctuations of H content, (ii) a high mass density and (iii) the coexistence of highly strained crystalline phases with a relaxed amorphous matrix. Unexplained optoelectronic properties and metastability phenomena can also be accounted for by this picture.

1. Introduction

Recently many efforts have been focused on hydrogenated amorphous silicon (a-Si:H) materials deposited 'on the edge of crystallinity' due to their promising potential for new generations of low cost optoelectronic and microelectronic devices [1–3]. In particular it has been shown that efficient and stable p–i–n junction solar cells can be obtained by means of plasma-enhanced chemical vapour deposition (PECVD) where the intrinsic layer is elaborated with a material at the onset of microcrystallinity [4–6].

Hydrogenated polymorphous silicon (pm-Si:H) is such a nanostructured material obtained by PECVD when running the plasma close to powder formation [1]. This material can be deposited at substrate temperatures (T_S) as low as 150 °C by using silane strongly diluted

in hydrogen, argon or helium [7, 8]. Intrinsic pm-Si:H exhibits a low defect density and an improved stability against light-induced degradation compared to the so-called 'standard' a-Si:H [9–11]. However, the precise structure of pm-Si:H films remains elusive. Indeed, from a structural point of view it appears very difficult to distinguish such nanostructured materials from a-Si:H since the 'ordered' regions are very small (typically below 5 nm) and highly diluted in the amorphous silicon matrix. X-ray diffraction (XRD) or Raman spectroscopy are usually not sufficiently sensitive techniques to emphasize the improved order of this type of film [12, 13]. High resolution transmission electron microscopy (HRTEM) and Raman spectroscopy have already revealed the presence of nanocrystallites embedded in the amorphous matrix of pm-Si:H films [12, 14] but only for a limited range of growth conditions. Consequently the link between the excellent optoelectronic properties and the structural properties of pm-Si:H is still poorly understood.

Optical spectroscopy techniques have proved to be powerful tools to investigate the structural properties of thin films. Thus the improved order of pm-Si:H films has been shown for a wide range of growth conditions by analysing visible–near-infrared (VIS–NIR) transmission spectra [15]. Careful modelling of spectroscopic ellipsometry data has also highlighted the peculiar structure of this material [16], namely nanometre sized crystallites embedded in an amorphous matrix. In this context the ability to probe hydrogen vibrational modes by Fourier transform infrared (FTIR) spectroscopy should shed some light on the structure of pm-Si:H films. Indeed earlier results of FTIR spectroscopy obtained on these films revealed a peculiar hydrogen bonding but this analysis was limited to the single stretching modes [12]. Mahan *et al* [13] observed a downshift of the wagging modes from 640 to 620 cm^{-1} for films deposited 'on the edge of crystallinity' ascribed to the presence of nanocrystallites. Therefore it is of significant interest to get a clearer picture of the H bonding in such a material.

In this paper we present a detailed study of IR absorption spectra of pm-Si:H films deposited at 150 °C by strong dilution of silane in hydrogen for a wide range of pressures. We show that a decomposition of the stretching absorption band into three modes is required, with the presence of a vibrational mode around 2030 cm^{-1}, to get a complete picture of hydrogen bonding in pm-Si:H films.

2. Experimental details

a-Si:H films were prepared by rf (13.56 MHz) glow discharge in a PECVD reactor by decomposition of pure silane at a substrate temperature (T_S) of 150 °C, a power density of 5 mW cm^{-2} and a total pressure of 5 Pa. Silane strongly diluted in hydrogen, i.e. SiH_4 diluted to 2% in H_2, was used as the reactant gas source to grow pm-Si:H films at $T_S = 150$ °C, a power density of 90 mW cm^{-2} and a total pressure which varied from 148 to 293 Pa. The deposition rate was of the order of 1 Å s^{-1} for both types of films.

FTIR spectroscopy measurements were performed on samples grown on c-Si substrates by using a Perkin Elmer Spectrum 2000 spectrometer in transmission mode with a resolution of 4 cm^{-1}. The spectra presented were averaged over 20 spectra and normalized to the transmission spectra of c-Si substrates. The absorption coefficients were determined by applying the method described in [17]. The integrated absorption I of the different modes observed are obtained by the usual formula $I = \int \alpha(\omega)/\omega \, d\omega$, where α is the absorption coefficient and ω is the wavenumber. The sample thickness was determined by correlating stylus profilometry measurements and the analysis of interference fringes in the VIS–NIR region of transmission spectra [15]. The latter measurements were performed on samples grown during the same run on Corning 1737 glass substrates. An excellent agreement was found for the thickness values obtained with both methods. The total bonded hydrogen content

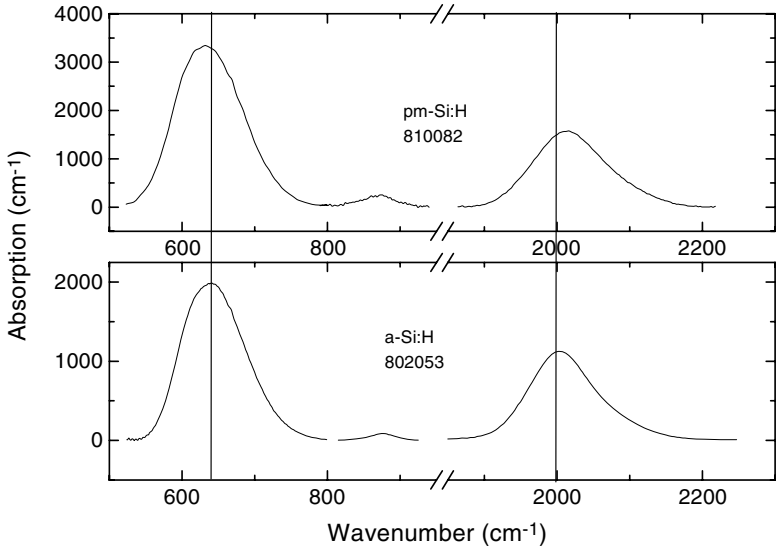

Figure 1. Infrared spectra for a pm-Si:H film and a a-Si:H film (upper and lower curves, respectively). See table 1 for the growth conditions. The vertical lines are a guide to the eye.

was deduced from the integrated absorption at ∼640 cm^{-1} by using the absorption strength value given by Beyer [18].

An optical technique was used to determine the substrate curvature and consequently the stress σ of the films. The substrate (c-Si) curvature radius R_c was deduced from the radius of the reflected wavefront of a laser beam ($\lambda = 632.8$ nm) from the sample into a camera, the incident beam being assimilated into a plane wave. The stress σ is deduced from Stoney's equation:

$$\sigma = \frac{E_s t_s^2}{6(1-\nu_s)t_f}\left(\frac{1}{R_c} - \frac{1}{R_0}\right) \tag{1}$$

where R_0 is the radius of curvature of the substrate before film deposition and E_s and ν_s are the Young's modulus and Poisson's ratio of the substrate, respectively. t_s and t_f are the thicknesses of the substrate and the film, respectively.

3. Results and discussion

3.1. Decomposition of the IR spectra

Figure 1 shows representative IR absorption spectra for a pm-Si:H sample and a a-Si:H sample. We can notice from figure 1 that (i) Si–H_2 bending modes are present for both kinds of material, (ii) the stretching absorption band is shifted to higher wavenumbers for pm-Si:H films and (iii) the absorption band at ∼640 cm^{-1} is shifted to lower wavenumbers for pm-Si:H films compared to a-Si:H.

In a-Si:H films it is well established that Si-H_2 bonds lead to bending modes in the 800–900 cm^{-1} wavenumber range. A doublet centred at ∼840 and ∼880 cm^{-1} is frequently observed for these vibrational modes [18]. The stretching band is usually decomposed into two modes centred at ∼2000 and ∼2090 cm^{-1}, respectively [18]. The low wavenumber mode is commonly attributed to isolated monohydrides and the high wavenumber mode either to

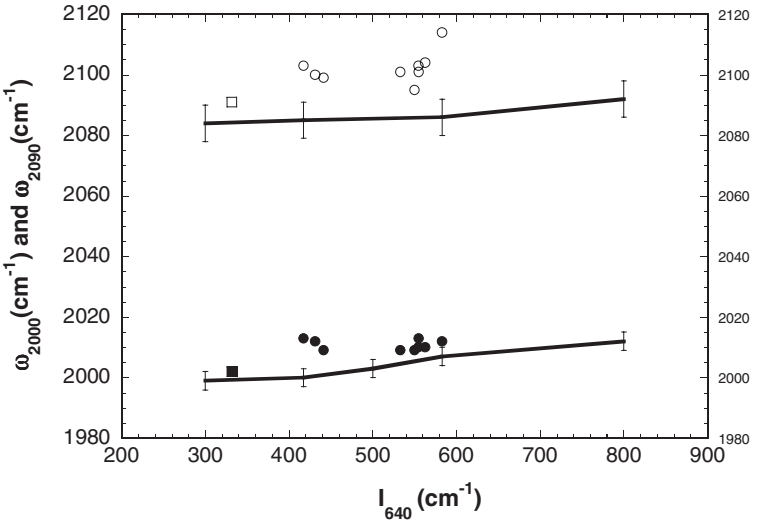

Figure 2. Peak wavenumbers for the modes at 2000 and 2090 cm^{-1} versus integrated absorption at 640 cm^{-1} for the pm-Si:H films (circles) and for the a-Si:H film (squares) obtained when decomposing the stretching absorption band into two modes. The lines are the mean results compiled by Beyer, the error bars representing the scattering of the data [18].

dihydrides or monohydrides overlaying the internal surface of microvoids [18]. The stretching band in our a-Si:H films is well reproduced, assuming a decomposition into two Gaussian functions centred at 2002 and 2092 cm^{-1} (see table 1). The microstructure parameter R defined as $R = I_{2090}/(I_{2000} + I_{2090})$, where I_{2000} and I_{2090} are the integrated absorption at 2000 and 2090 cm^{-1}, respectively, is close to 0.13, a typical value for a-Si:H films deposited at $T_S = 150\,^{\circ}$C [19]. Similarly the stretching band of pm-Si:H films was decomposed into two Gaussian functions corresponding to the modes observed in a-Si:H. Figure 2 shows the peak position of these modes versus absorption at 640 cm^{-1} (I_{640}) which is proportional to the hydrogen content. The full curves correspond to the wavenumbers compiled recently by Beyer for glow discharge films [18]. When increasing the hydrogen bonded content an increase of the peak wavenumber is usually found [18, 20]. This behaviour is commonly explained by the so-called induction effect model [21]. We can notice a clear departure from the range determined by Beyer for the peak wavenumbers in pm-Si:H films [18]. In addition the measured peak wavenumbers are significantly scattered despite the narrow distribution of bonded hydrogen content in these samples. At this early stage we should point out that in pm-Si:H films most of the hydrogen is bonded to silicon atoms in the amorphous matrix since the fraction of 'ordered' regions is fairly low (this point will be addressed in more detail below) [12, 14]. Therefore we expect a stretching mode at $\sim$2000 cm^{-1} associated with isolated Si–H bonds as well as an absorption band centred at $\sim$2090 cm^{-1} due to the presence of bending modes. We also stress the fact that the analysis of ellipsometry measurements has proved pm-Si:H films to be almost free of microvoids [16]. This latter point is in agreement with the high mass densities found for this material [22]. Therefore we can safely conclude that in these samples the absorption band at 2090 cm^{-1} is mainly due to the presence of dihydrides.

From the previous analysis it appears that the decomposition of the stretching absorption band into two Gaussian functions is not convincing physically for pm-Si:H films. On the other hand, a decomposition of the stretching absorption band into three Gaussian functions reveal a new mode centred at $\sim$2030 $\pm$ 3 cm^{-1}. Such a decomposition is presented in figure 3 and

Table 1. Parameters deduced from the analysis of the IR spectra. I_{640}, I_{880}, I_{2000}, I_{2030} and I_{2090} are the integrated absorption of the different modes, values in brackets being absolute errors from the fits. ω_{2000}, ω_{2030} and ω_{2090} are the peak wavenumbers obtained by decomposition of the stretching band into two or three Gaussian functions and ω_{640} is the peak wavenumber of the mode observed close to 640 cm^{-1}, the maximum error being ± 3 cm^{-1}.

Samples	Pressure (Pa)	C_H (%)	I_{640} (cm^{-1})	ω_{640} (cm^{-1})	I_{880} (cm^{-1})	I_{2000} (cm^{-1})	ω_{2000} (cm^{-1})	I_{2030} (cm^{-1})	ω_{2030} (cm^{-1})	I_{2090} (cm^{-1})	ω_{2090} (cm^{-1})
a-Si:H 802053	5	12.2	332 (0.3)	640.5	3.9 (0.2)	56 (0.4)	2002	—	—	8.3 (0.2)	2092
810081	160	18.3	533.3 (0.2)	628	10.9 (0.4)	54.2 (1.6)	2000	15.7 (0.8)	2027	24.9 (0.3)	2086
810082	202	19.6	582.9 (0.4)	630.5	9.1 (0.3)	58.8 (0.3)	1997	19 (0.4)	2030	19.5 (0.1)	2085
810083	239	18.9	555 (0.2)	628.7	8.5 (0.2)	66.2 (0.2)	1998	15 (0.3)	2027	13.6 (0.1)	2085
810092	266	18.9	554.8 (0.3)	624.1	9.3 (0.2)	64.1 (0.4)	1998	12.9 (0.5)	2030	13.6 (0.1)	2085
810093	293	18.8	550 (0.1)	630.5	10.5 (0.1)	57.4 (0.2)	2000	12.7 (0.3)	2026	16.4 (0.1)	2085
901251	207	19.1	562.7 (0.2)	627	12.1 (0.1)	79.5 (0.6)	1998	16.9 (0.6)	2027	19.8 (0.1)	2086
901261	173	15.6	441.6 (0.3)	630.3	12.2 (0.2)	58.3 (0.6)	1998	19.9 (0.6)	2030	21.6 (0.1)	2085
901262	200	14.9	417.7 (0.3)	631.5	10.6 (0.2)	55.5 (0.2)	1998	16.4 (0.2)	2026	19.2 (0.1)	2088
901271	148	15.3	431.2 (0.4)	622.8	11.3 (0.3)	56.4 (0.2)	1997	15.8 (0.3)	2028	16.1 (0.1)	2086

compiled in table 1 for all the samples studied. It can be seen that the values of ω_{2000} and ω_{2090} compiled in table 1 agree well with the results of Beyer [18].

Though this procedure gives excellent results it cannot serve as a sufficient criterion to validate this approach. However, by considering that the absorption band at 2090 cm^{-1} is only due to dihydrides (cf the earlier comment) the integrated absorption at 880 cm^{-1} (I_{880}) versus integrated absorption at 2090 cm^{-1} (I_{2090}) should verify the well established ratio between these two quantities [23]. This ratio is presented in figure 4 for all the pm-Si:H films studied in this work together with various results from the literature for samples deposited either by rf magnetron sputtering [24] or by PECVD [25]. The full line has a slope equal to 0.42, in very good agreement with the ratio I_{880}/I_{2090} found in previous studies [25]. We also report in figure 4 the dependence of I_{880} versus I_{2090} deduced from a decomposition of the stretching band into two Gaussian functions only. Clearly these points do not follow the same trend.

Another interesting feature of these IR spectra is the shift of the wagging band toward lower wavenumbers (see table 1). In pure a-Si:H films the position of this band remains almost unchanged [18]. On the other hand, a wagging mode wavenumber close to 620 cm^{-1} has been reported by Mahan *et al* [2] for films deposited 'on the edge of crystallinity'. Similarly we can notice a clear downshift of the wavenumber for the wagging modes when going from amorphous to microcrystalline samples in the spectra shown in [26]. Then the analogy with the mode observed at 620 cm^{-1} in hydrogenated c-Si by Wagner and Beyer [27] appears straightforward.

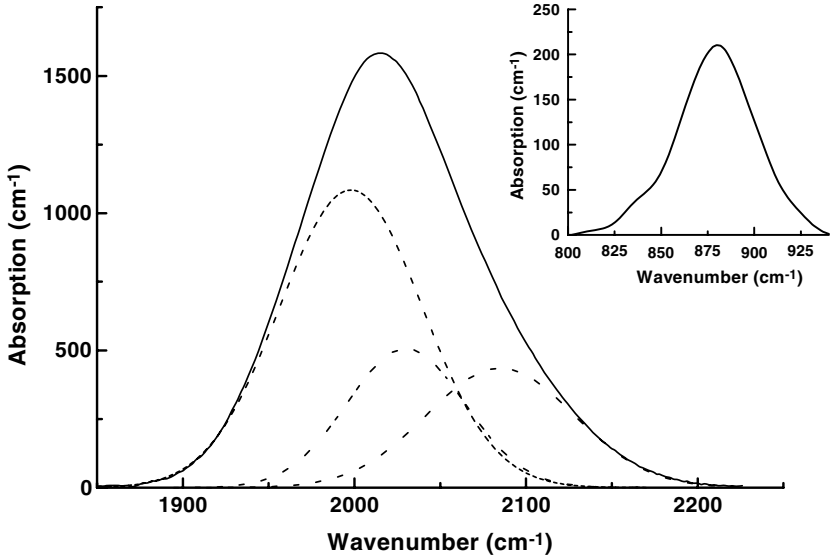

Figure 3. Decomposition of the stretching absorption band for a pm-Si:H film into three modes (broken curves). The inset shows the bending absorption band obtained for the same film.

3.2. Links between hydrogen bonding, residual stress, structural properties and metastability in pm-Si:H films

3.2.1. Brief overview of specific Si–H stretching modes in nanocrystalline-like and highly hydrogenated silicon materials. Several results from the literature can help us to elucidate the hydrogen configuration related to this mode observed at 2030 cm^{-1} in pm-Si:H films.

Von Keudell and Abelson [28] reported a mode at 2033 cm^{-1} attributed to clustered Si–H groups in platelet-like configurations. These groups are formed during the growth by insertion of hydrogen atoms into strained Si–Si backbonds. Marra *et al* [29] found a bulk mode close to 2050 cm^{-1} occurring during the growth of hydrogenated nanocrystalline silicon by PECVD. These authors suggest that this component results from Si–H bonds located at the amorphous–crystalline interface since this feature could be resolved only for films having a crystalline component. Si–H bulk modes have been identified by Fujiwara *et al* [30] at wavenumbers ranging from 2024 to 2030 cm^{-1} when exposing thin a-Si:H films to H_2 plasma, leading to the nucleation of μc-Si:H. In a review of the experimentally observed stretching bands, Deak *et al* [31] attributed the modes in the 2030–2066 cm^{-1} range to (Si–Si–Si)Si–H complexes. These authors mentioned that the band observed at 2030 cm^{-1} disappears upon annealing for temperatures as low as 300 °C. The analogy with pm-Si:H films is then straightforward since we observed in a previous study the disappearance of this mode occurring at 2030 cm^{-1} for temperatures close to 350 °C [22].

The so-called polarized medium model has been applied with success by Cardona [32] to account for the shift of hydrogen wavenumbers observed either in bulk hydrogenated crystalline or amorphous silicon. By using a similar approach it was concluded in [28] that the mode at 2033 cm^{-1} ascribed to hydrogen platelets should lie between the isolated Si–H bond mode at 2000 cm^{-1} and the surface Si–H mode at 2100 cm^{-1}. The higher wavenumber observed in [29] can also be explained within this framework. Indeed we expect an IR mode increasing toward the wavenumber of the surface Si–H modes when increasing the size of these platelets.

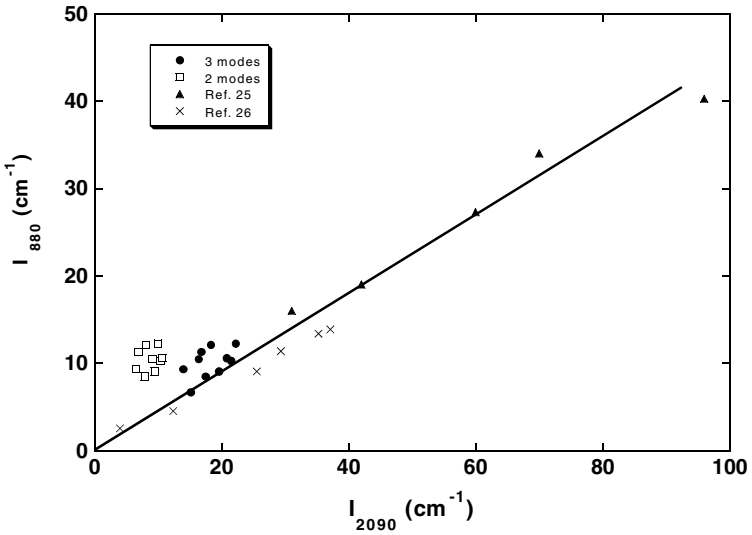

Figure 4. Integrated absorption at 880 cm^{-1} (I_{880}) versus integrated absorption at 2090 cm^{-1} (I_{2090}) including the deconvolution of the stretching band into two or three modes (see the text for details). The results obtained for pm-Si:H films are presented together with various results from the literature [25, 26]. The line is a guide to the eye.

This is consistent with the larger crystallite size in the films studied in [29] compared to pm-Si:H films [12]. Moreover as pointed out in [28] small platelets should not lead to open voids whereas larger platelets will do. Consequently in the latter case these highly hydrogenated films should exhibit an increased porosity, i.e. when going from pm-Si:H to μc-Si:H the size of both crystalline grains and hydrogen platelets located at the grain boundary should increase, leading to open voids and a decrease of the mass density. Such a behaviour has been reported for pm-Si:H films following studies performed both by spectroscopic ellipsometry [16] and mass density measurements [22].

Though the presence of hydrogen platelets can account for this additional mode around 2030 cm^{-1} this is not the only possible explanation. Indeed, by considering the induction model [21], Dutta and Chaudhuri [33] calculated Si–H wavenumbers up to 2024 cm^{-1}. Moreover, by taking into account the repulsive interaction between H atoms the wavenumber shifts of Si–H groups can be extended beyond what is predicted by the induction model [34]. However, we will see below that H complexes, such as platelets, are likely to be present in our films and this will explain numerous experimental results for pm-Si:H films.

3.2.2. Assignment of the third stretching mode in pm-Si:H films and description of the ordered regions. From the previous analyses we assign the stretching mode at 2030 cm^{-1} to Si–H groups bonded at the interface between 'ordered' regions and the amorphous silicon matrix. As far as hydrogen platelets are concerned the most probable configuration for Si–H groups would be $[H_2^*]_n^D$ complexes or $[2Si–H]_n$ complexes with H_2 molecules inserted in the interstitial region [35]. Moreover both nuclear magnetic resonance (NMR) [36] and multiple reflections infrared spectroscopy [37] indicate that H_2 molecules are present in a-Si:H. Su *et al* [36] suggested for their films exhibiting a more ordered structure that H_2 molecules are trapped in small crystalline regions or at crystalline–amorphous boundaries. Such a picture has been invoked to account for several metastability phenomena observed in a broad class of silicon-

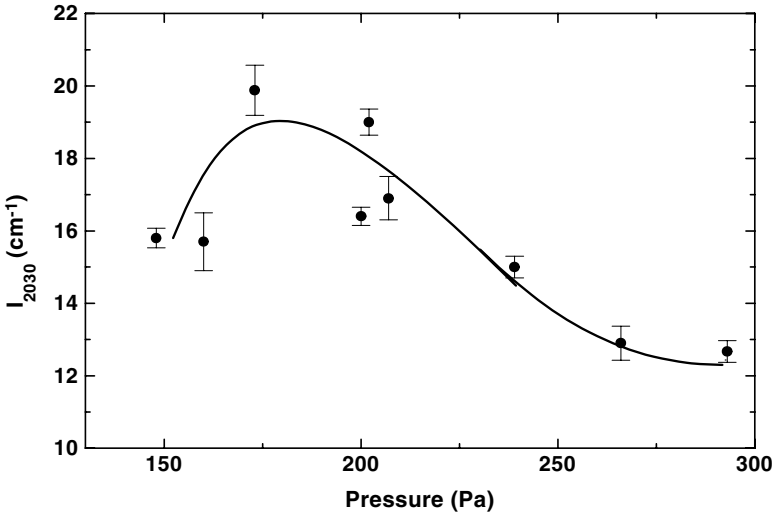

Figure 5. Integrated absorption at 2030 cm^{-1} versus deposition pressure. The error bars are issued from the decomposition of the stretching band into three modes. The curve is a guide to the eye.

based materials [38]. It could also explain the increase of the compressive strains observed in pm-Si:H films with respect to a-Si:H films (see below). Moreover recent NMR results have given direct evidence of the role of paired hydrogen in the creation of light-induced metastable defects [39].

Though further work is needed to elucidate the precise nature of these Si–H groups in pm-Si:H films, (i.e. do we have monohydride chains or platelet-like H complexes?) H-rich regions are likely to be present in our films, thus favouring the creation of H_2 molecules. This view is supported by the large potential fluctuations [40] and by the low-temperature exodiffusion peak found in pm-Si:H films [22].

Let us now show that the assignment of the mode at 2030 cm^{-1} to specific Si–H bond configurations is consistent with a great variety of results. The evolution of the integrated absorption at 2030 cm^{-1} with deposition pressure is reported in figure 5. I_{2030} exhibits a maximum for pressures in the 170–200 Pa range. Now a careful analysis of ellipsometry data showed that the maximum concentration of crystallites in pm-Si:H films is likely to occur at a pressure of 170 Pa [14], a pressure lying in the range where pm-Si:H samples exhibit the best transport and optoelectronic properties [10, 12]. Thus these improved properties should be closely linked to the presence of such ordered nanostructures. However, one question remains open: can we ascribe these improved properties directly to the crystallites (or ordered regions) or is it due to an amorphous matrix with an improved medium range order (MRO) with respect to a-Si:H? This issue will be discussed further below.

The presence of crystallites in pm-Si:H samples deposited at 160 Pa has been demonstrated by HRTEM [8, 12, 14] and Raman spectroscopy [12]. HRTEM revealed isolated nanoparticles having the diamond structure with a diameter ranging from 3 to 5 nm [12]. A mean crystallite diameter of 4 nm was deduced from the corresponding Raman spectra [12]. Assuming that the hydrogen leading to the mode at 2030 cm^{-1} is located on the crystallite surface we can roughly estimate the density of crystallites from their mean diameter. For this purpose we need to know the value of the absorption strength A_{2030} to determine the atomic hydrogen density vibrating at this wavenumber. In [28] the same factor was used for all the stretching modes and Beyer [18] argued that for a given hydrogen content the same factor should apply. Therefore

we used the value given in [41] for a hydrogen content of 18%, i.e. $A = 1.03 \times 10^{20}$ cm^{-2}. By considering a coverage density of the (111) c-Si surface by hydrogen atoms of 10^{15} cm^{-2} [29], we deduced a density of crystallites equal to $(3.2 \pm 0.2) \times 10^{18}$ cm^{-3}, corresponding to a crystalline fraction of $10.7\% \pm 0.6\%$. This value is in reasonable agreement with the 9% deduced from Raman spectroscopy [12]. Knowing that we assumed a spherical shape for all the crystallites, we neglected their size distribution and moreover we did not consider the various crystalline phases that can be present (see point (iii) of the discussion).

For the samples grown at higher pressures both Raman spectroscopy and HRTEM techniques failed to show the signature of crystallites. However, this point is not incompatible with the observation of a mode at 2030 cm^{-1}. It simply means that the ordered regions become too small in this range of pressures to be detected. Such a picture is in agreement with the departure from powder formation conditions observed when increasing the gas pressure [7]. By ordered regions is meant topologically crystalline phases existing in pm-Si:H films for the whole range of deposition pressures. In this way this approach is consistent with the increase of the MRO found by HRTEM analysis for pm-Si:H samples [16]. These regions are generally identified as paracrystallites [42, 43] and have been invoked to explain the continuous increase of the MRO found when going from amorphous toward polycrystalline materials [44]. Paracrystallites are generally assimilated to highly strained crystallites with a diameter below 3 nm, embedded in a disordered matrix, deformed by the elastic relaxation of the grain boundary stress. The common signature of this type of material in XRD measurements is amorphous-like [42]. Thus, even if the conventional experimental techniques used to characterize structural properties failed to detect ordered regions in this type of film, the vibrational mode at 2030 cm^{-1} appears as a strong signature of the presence of paracrystallites (in pm-Si:H films deposited at high pressure) and/or nanocrystallites (in pm-Si:H films deposited at low pressure). As pointed out in [42] the structure of these paracrystallites is not necessarily that of bulk diamond. This is likely to occur in pm-Si:H films due to the high compressive stress measured (see below). Experimentally it is well supported by the numerous crystalline structures which have been identified in these films by means of HRTEM [8, 12, 14]. It must be emphasized that the structure of pm-Si:H films is homogeneous on their whole thickness, as depicted in [16], and thus HRTEM studies performed on very thin films deposited for this purpose are relevant.

Due to their large free energy paracrystallites are expected to undergo a transition upon annealing toward an amorphous phase like the continuous random network at temperatures well below the crystallization temperature of Si [42]. We observed such a behaviour, although indirectly, by performing isochronal annealing followed by FTIR measurements [22]. It was shown that the mode at 2030 cm^{-1} disappears at temperatures close to 350 °C and the low temperature exodiffusion peak characteristic observed was ascribed to the peculiar Si–H bonding at the boundaries of the ordered zones. Moreover, by considering a thermodynamic criterion the smallest crystallite size having the diamond lattice structure was determined to be 30 Å [45], this limit being extended to 20 Å if the crystallites are under large compressive stress. Below these limits the crystallites are highly unstable due to lattice expansion. Thus, by assuming that the large compressive stress due to H-rich regions stabilizes the ordered structures, they should evolve toward an amorphous phase when releasing the hydrogen which leads to a low temperature exodiffusion peak [18]. This picture is fully consistent with the results obtained by Kim *et al* [46] for a-Si:H films deposited using silane highly diluted in hydrogen where the structural disorder increased drastically shortly after the observation of a low temperature hydrogen exodiffusion peak.

3.2.3. Links between residual stress and microscopic structure in pm-Si:H films. Intrinsic compressive stress values of 700 and 800 MPa were measured for pm-Si:H films deposited

at 170 and 240 Pa, respectively. As the thermal stress arising from the mismatch between the thermal expansion coefficient of the film and that of the substrate is of the order of 20 MPa in our case, it can be neglected [47]. These stress values are in good agreement with those found in the literature [48, 49] for films obtained by decomposition of silane highly diluted in H_2. It is also close to the intrinsic stress values of 900 MPa reported in [26] for films grown at the amorphous/microcrystalline silicon transition. However, the intrinsic stress values in pm-Si:H films are significantly larger than those measured in conventional PECVD a-Si:H films ranging from 150 to 300 MPa [26, 47].

We now reconcile the high stress values found in pm-Si:H films with the microscopic structure described above. We first remember that the mass density values of pm-Si:H films are significantly larger than those expected when assuming a monovacancy model [22]. It means that high pressure phases of Si are likely to be present in our films. This is reinforced by the increase of the Penn gap (E_P) in these films compared to a-Si:H films [15]. Indeed E_P can be seen as a global measure of the disorder and its increase could also be attributed to the presence of high pressure phases of Si. H-rich regions with trapped H_2 molecules would explain in a natural manner the latter results as well as the great variety of crystalline structures observed by HRTEM in this material. Indeed previous studies [37, 50] showed that H_2 molecules inserted in a silicon network are under high pressure, typically around 200 MPa, and Graebner *et al* [51] have found that H_2 molecules are clustered in groups of two or more rather than isolated. Moreover the pressure build-up in $[H_2^*]_n^D$ complexes has been estimated to be of the order of 2–4 GPa [52] and decreases to 1 GPa when accompanied by lattice dilatation leading then to $[2Si–H]_n$ complexes with H_2 molecules [35]. Thus the increase of the gas pressure in the vicinity of the ordered regions is likely to lead to an increase of the macroscopically observable stress. Since pm-Si:H films are almost free of microvoids [16] and have a low dangling bond density [10], the stress accumulated mainly at the interfaces cannot be easily released. This picture explains why pm-Si:H samples did not withstand annealing at 350 °C without forming craters and peeling, this temperature coinciding with the disappearance of the mode at 2030 cm^{-1} and the observation of the low temperature exodiffusion peak [22].

When studying the incubation layer at the early stage of μc-Si:H growth, a strong correlation between compressive stress and density of Si–H complexes was noticed [53], both quantities increasing in the same manner, thus favouring the μc-Si:H nucleus density. In order to release the compressive stress the creation of microvoids is needed, leading thus to a material with an increased porosity. This is precisely what happens when decreasing the deposition pressure. Indeed, for deposition pressures below 106 Pa the resulting material is microcrystalline and the mass density drops drastically [22]. It is well known that before microcrystalline growth occurs a thin incubation layer is grown [3, 54]. This layer is often referred to as protocrystalline silicon and structurally resembles pm-Si:H films although slight differences have been shown by ellipsometry [54]. Protocrystalline silicon is a dense material [54] which can only be deposited up to a given critical thickness, beyond which a transition to μc-Si:H is observed [3, 54]. Koh *et al* [3] attributed the transition from protocrystalline silicon to μc-Si:H growth to higher-order zones present in the protocrystalline silicon layer and/or to H-induced stress build-up due to trapped H_2 molecules. It is likely that the stress in protocrystalline silicon layers is even larger than in pm-Si:H films, thus explaining why thick protocrystalline silicon layers cannot be grown, contrary to pm-Si:H material [54], this view being consistent with measurements of [55].

Now we address the various crystalline silicon phases observed by HRTEM in pm-Si:H films. Structures such as the diamond structure [12], the hexagonal close packed structure (a metastable phase of Si), and cubic fcc and bc8 [8] were identified. The latter phases are usually given as unstable polytypes of Si obtained under high pressure [56]. Consequently

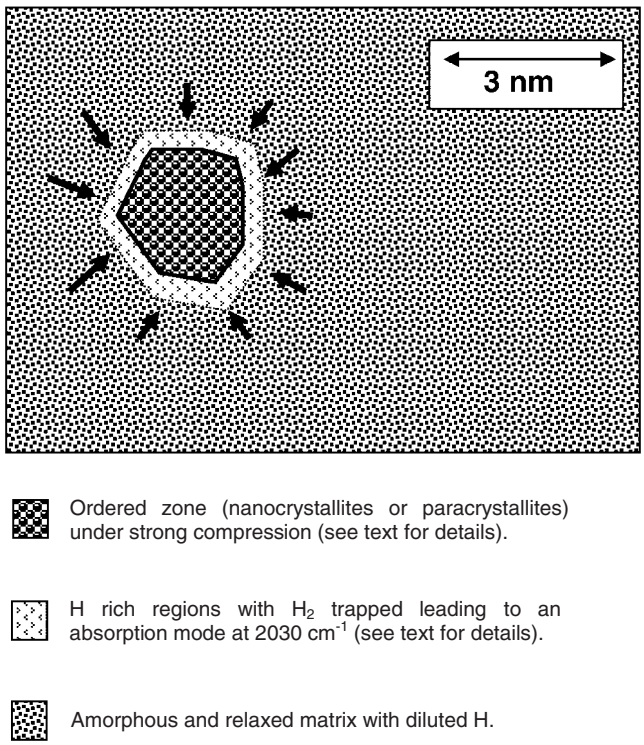

Figure 6. Simple picture of the structure of pm-Si:H films.

the ordered structures in pm-Si:H films are likely to be under high pressure. The pressure increase in these films can thus be explained by the presence of H-rich regions and by the coexistence of two Si phases, namely amorphous and crystalline. This is in agreement with calculations of the amorphous–crystal interface in Si showing that the crystalline phase was under biaxial compression [57]. However, a considerable pressure, say several gigapascals, should exist to obtain the various crystalline structures observed. We can reasonably assume that $[H_2{}^*]_n^D$ complexes or $[2Si–H]_n$ complexes with inserted H_2 molecules can locally supply such pressures. Figure 6 gives a picture of the pm-Si:H structure consistent with the results quoted above.

3.2.4. Implications on optoelectronic properties and metastability phenomena. Several models have been proposed to explain metastability phenomena in hydrogenated silicon thin films. Among them recent models [38, 58] are consistent with the numerous observations issued from NMR, ESR, IR or volume expansion measurements (see [38] and [58] and references therein). These models invoke paired hydrogen to explain defect creation. Whereas Powell *et al* [58] stipulate that these paired hydrogen atoms are located in non-clustered hydrogen regions and are coming from SiHHSi complexes where the H atoms are in tetrahedral sites, Longeaud *et al* [38] assume that the defect creation is mediated via H_2 molecules in tetrahedral-like (T-like) sites and that defects are created close to H-rich regions. Consequently we can wonder whether the metastable defects are created in the amorphous tissue or nearby to the ordered zones where H-rich regions are present. It appears that recently a clear correlation was shown between the values of the normalized photoconductivity ($\eta\mu\tau$ product) and the

proximity of H_2 molecules located in T-like sites to light-induced defects [59]. In this latter work the highest $\eta\mu\tau$ product was obtained for films deposited by H dilution of silane with the highest H_2 molecule content. It was thus concluded that H_2 molecules in T-like sites are located in regions controlling the optoelectronic properties. In the light of these results we can assume that defects are mostly created in H-rich regions, contrary to the picture proposed in [58].

Based on the previous analysis we assume that H_2 molecules trapped in H-rich regions are present in the vicinity of the ordered zones to explain both the large values of the compressive stress and the peculiar crystalline structures observed in pm-Si:H films. Thus, following the results of [59] the optoelectronic properties would be controlled by these regions. Even if we cannot exclude the presence of defects in the amorphous tissue, we will show that this picture is consistent with the experimental results of transport and metastability properties in pm-Si:H films as well as other results from the literature.

In a previous study [9] we highlighted the peculiar behaviour of pm-Si:H films occurring during light-soaking (LS), i.e. a very rapid and large degradation of both the $\eta\mu\tau$ product and defect density. However, in the fully light-soaked state the best pm-Si:H films still have a lower (higher) defect density ($\eta\mu\tau$ product) compared to standard a-Si:H films in the annealed/as-deposited state. This behaviour can readily be explained by assuming the creation of metastable defects in the vicinity of H-rich regions as claimed in [38]. Indeed, as mentioned previously these zones are under large compressive stress and Wehrspohn *et al* [60] showed that an increase of the compressive stress leads to an increase of (i) the defect creation rate and (ii) the magnitude of defects created. This occurs due to the lowering of the energy barrier for defect creation and is fully consistent with our previous findings [9]. Moreover a decrease of the MRO upon LS was found in films containing paracrystalline structures [61]. This phenomenon was explained by the creation of defects in the vicinity of more ordered zones where considerable strains and weak bonds coexist, a picture in agreement with the assumptions established for our films. In addition a phenomenological model was proposed recently to account for the decrease of the MRO [62]. The authors suggested that light-induced changes occur at the boundary of more ordered regions, thus encroaching on these zones, a picture again fully consistent with our assumptions.

Another intriguing result concerning pm-Si:H films is the temperature dependence of the steady-state defect density (N_{SS}) upon LS. We found an increase of N_{SS} with temperature [9] whereas the opposite behaviour is generally reported for a-Si:H (see [63] and references therein). Since the temperature dependence of N_{SS} is a balance between activation energies of the annealing and creating defect terms under illumination [63], a very low activation energy of the annealing term under illumination is required to explain these results. We can thus wonder how to reconcile the temperature dependence of N_{SS} with the creation of H_2 molecules occurring during LS experiments. First the stress exerted on H_2 molecules trapped in interstitial sites will depend greatly on the space available [38]. It can thus explain the irreversible metastable phenomena observed in pm-Si:H films since the less constrained H_2 molecules would need an amount of thermal energy too large to be dissociated and to passivate the dangling bonds. However, molecular dynamics simulations highlighted that H_2 molecules located near strained Si–Si bonds dissociate without an energy barrier [64]. As large strains are expected in H-rich regions, the N_{SS} dependence with temperature can be explained by the spontaneous dissociation of H_2 molecules with the lowest degree of freedom created during LS. This point could also explain the surprising results of [65] where a partial recovery of photodegradation in a-Si:H (of about 10%) at room temperature was reported, assuming that some defect passivation occurs due to the spontaneous dissociation of strained H_2 molecules. Moreover Estreicher *et al* [64] pointed out that H_2 molecules can also be dissociated under

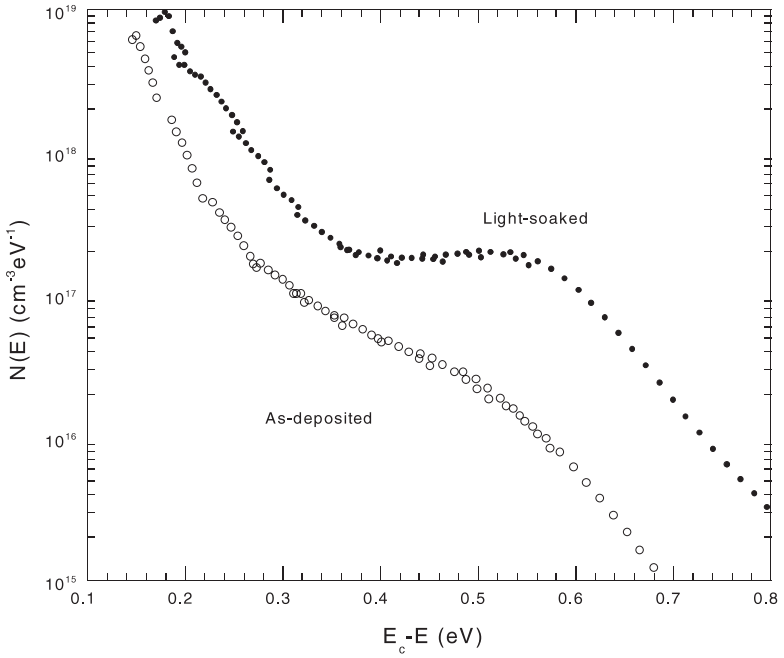

Figure 7. Density of states at 300 K deduced from MPC technique for the film 810083 obtained in the as-deposited state and after LS at 353 K under a flux of 300 mW cm^{-2} until a steady state was reached.

illumination. Thus during LS there will be a balance between creation and annihilation of H_2 molecules, leading to a steady-state defect density. It can thus also explain why the recovery of the pm-Si:H film properties after light-induced degradation is enhanced under illumination [9, 63].

Finally we address the broadening of the conduction band tail (CBT) observed for pm-Si:H films (see figure 7) [66]. This phenomenon can also be explained within the picture described above together with the theoretical study on the nature of band tail states in a-Si:H developed in [67]. In this latter work it was reported that CBT and valence band tail states (i.e. weakly bonded states) are due to long and short bonds, respectively. Following [38], during LS H atoms are inserted in bond-centred and antibonding positions before gathering to form H_2 molecules. We can then reasonably assume that Si–Si bonds are undergoing a length increase after releasing bond centred H atoms. Moreover since storing H_2 molecules necessitates some space it explains in a natural manner the commonly observed volume expansion during LS [68]. However, we must note that the increase of the CBT has been highlighted by means of the modulated photocurrent (MPC) technique. With this technique the probed quantity is proportional to the density of states (DOS)–electron capture cross section (σ_c) product. Thus an increase of σ_c values cannot be excluded. Indeed it has been established that σ_c increases for deep defects during LS [69, 70] which could also be the case for CBT states. In this model it was postulated that this increase of σ_c results from an increase of the local strains near the created defects [70]. In this framework it has been possible to explain the different behaviour of the $\eta\mu\tau$ and defect density kinetics upon LS. Thus whatever the origin of the increase of the MPC signal in the CBT region, i.e. either an increase of σ_c or simply an increase of the DOS or even an increase of both quantities, the nature of this evolution is likely to be due to a modification of the local strains.

To complete our analysis of metastability phenomena in pm-Si:H films we cannot exclude the presence of charged defects in the as-deposited state and their creation upon LS. As stated in [71] the presence of charged defects is more likely in inhomogeneous films where potential fluctuations are large, which is the case for pm-Si:H films [40]. Several experimental results revealed the presence of charged defects (see [71] and references therein) which have also been invoked to explain the kinetics of light-induced changes in protocrystalline films [72]. However, when invoking charged defects as the main ones in pm-Si:H material we would expect a significant increase (several orders of magnitude) of the electron capture cross section values compared to those measured experimentally [73].

4. Conclusion

The necessity to decompose the stretching modes into three bands with a band centred at $\sim$2030 cm^{-1} has been pointed out when analysing hydrogen bonding from FTIR spectra of pm-Si:H films. This latter band has been related to the peculiar nanostructure of these films and has been attributed to Si–H groups located at the boundary between the amorphous matrix and ordered regions identified either as metastable paracrystallites or nanocrystallites. This assignment is consistent with data of H evolution upon annealing. The intensity dependence of this stretching mode with the deposition conditions is also in good agreement with previous results obtained by using more sophisticated techniques and analysis. Whereas Raman spectroscopy or HRTEM failed to highlight the peculiar structure of pm-Si:H films for most of the growth conditions, it has been possible to detect relatively small gradual structural differences in this material by looking at the hydrogen bonding by FTIR spectroscopy.

As a result the structure of pm-Si:H films has been described as a two-domain material where dense and ordered zones under high compressive stress surrounded by H-rich regions are embedded in an amorphous tissue with higher hydrogen dilution. From our previous results and those from the literature we assume that defects created upon LS are mainly located in the vicinity of the ordered zones and that both transport and optoelectronic properties are controlled by these defects. We conclude that the enhanced stability of this material is likely to be linked to the peculiar nanostructure of this material rather than to the hydrogen content. This picture explains in a natural manner the higher mass density, the large potential fluctuations and the increase of MRO of pm-Si:H films compared to a-Si:H. We have also highlighted another relevant physical parameter, namely intrinsic stress, which seems to play a major role in metastability phenomena.

Acknowledgments

We gratefully acknowledge Dr P Roca i Cabarrocas for providing the samples and Dr C Longeaud for fruitful discussions and for providing the data of figure 7. This work was supported by Centre National de la Recherche Scientifique and Agence pour le Développement et la Maîtrise de l'Energie (ECODEV programme).

References

[1] Roca i Cabarrocas P 2000 *J. Non-Cryst. Solids* **266–269** 31
[2] Mahan A H, Beyer W, Williamson D L, Yang J and Guha S 2000 *Phil. Mag. Lett.* **80** 647
[3] Koh J, Ferlauto A S, Rovira P I, Wronski C R and Collins R W 1999 *Appl. Phys. Lett.* **75** 2286

[4] Roca i Cabarrocas P, Hamma S, St'ahel P, Longeaud C, Kleider J P, Meaudre R and Meaudre M 1997 *Proc. 14th European Photovoltaic Solar Energy Conf. and Exhibition (Barcelona, 1997)* ed H A Ossenbrink, P Helm and H Ehmann (Stephens: Bedford) p 1444
[5] Guha S, Yang J, Williamson D L, Lubianiker Y, Cohen J D and Mahan A H 1999 *Appl. Phys. Lett.* **74** 1860
[6] Yang J, Banerjee A and Guha S 1997 *Appl. Phys. Lett.* **70** 2975
[7] Roca i Cabarrocas P 1998 *Mater. Res. Soc. Symp. Proc.* **507** 855
[8] Viera G, Mikikian M, Bertran E, Roca i Cabarrocas P and Boufendi L 2002 *J. Appl. Phys.* **92** 4684
[9] Butté R, Meaudre R, Meaudre M, Vignoli S, Longeaud C, Kleider J P and Roca i Cabarrocas P 1999 *Phil. Mag.* B **79** 1079
[10] Meaudre M, Meaudre R, Butté R, Vignoli S, Longeaud C, Kleider J P and Roca i Cabarrocas P 1999 *J. Appl. Phys.* **86** 946
[11] Kleider J P, Longeaud C, Gauthier M, Meaudre M, Meaudre R, Butté R, Vignoli S and Roca i Cabarrocas P 1999 *Appl. Phys. Lett.* **75** 3351
[12] Butté R, Vignoli S, Meaudre M, Meaudre R, Marty O, Saviot L and Roca i Cabarrocas P 2000 *J. Non-Cryst. Solids* **266–269** 263
[13] Mahan A H, Yang J, Guha S and Williamson D L 1999 *Mater. Res. Soc. Symp. Proc.* **557** 269
[14] Fontcuberta i Morral A, Brenot R, Hamers E A G, Vanderhaghen R and Roca i Cabarrocas P 2000 *J. Non-Cryst. Solids* **266–269** 48
[15] Vignoli S, Butté R, Meaudre R, Meaudre M and Roca i Cabarrocas P 1999 *J. Phys.: Condens. Matter* **11** 8749
[16] Fontcuberta i Morral A, Hofmeister H and Roca i Cabarrocas P 2002 *J. Non-Cryst. Solids* **299–302** 284
[17] Maley N 1992 *Phys. Rev.* B **46** 2078
[18] Beyer W 1999 *Semiconductors and Semimetals* vol 61, ed N H Nickel (San Diego, CA: Academic) p 165
[19] Roca i Cabarrocas P, Djebbour Z, Kleider J P, Longeaud C, Mencaraglia D, Sib J, Bouizem Y, Thèye M L, Sardin G and Stoquert J P 1992 *J. Physique* I **2** 1979
[20] Mahan A H, Gedvilas L M and Webb J D 2000 *J. Appl. Phys.* **87** 1650
[21] Lucovsky G 1979 *Solid State Commun.* **29** 571
[22] Vignoli S, Fontcuberta i Morral A, Butté R, Meaudre R and Meaudre M 2002 *J. Non-Cryst. Solids* **299–302** 220
[23] Lucovsky G, Nemanich M J and Knights J C 1979 *Phys. Rev.* B **19** 2064
[24] Touir H, Zellama K and Morhange J F 1999 *Phys. Rev.* B **59** 10076
[25] Manfredotti C, Fizzoti F, Boero M, Pastorino P, Polesello P and Vittone E 1994 *Phys. Rev.* B **50** 18046
[26] Kroll U, Meier J, Shah A, Mikhailov S and Weber J 1996 *J. Appl. Phys.* **80** 4971
[27] Wagner H and Beyer W 1983 *Solid State Commun.* **48** 585
[28] von Keudell A and Abelson J R 1998 *J. Appl. Phys.* **84** 489
[29] Marra D C, Edelberg E A, Naone R L and Aydil E S 1998 *J. Vac. Sci. Technol.* A **16** 3199
[30] Fujiwara H, Toyoshima Y, Kondo M and Matsuda A 2000 *Mater. Res. Soc. Symp. Proc.* **609** A2.1.1
[31] Deak P, Snyder L C, Heinrich M, Ortiz C R and Corbett J W 1991 *Physica* B **170** 253 and references therein
[32] Cardona M 1983 *Phys. Status Solidi* b **118** 463
[33] Dutta G N and Chaudhuri P 2003 *J. Phys. D: Appl. Phys.* **36** 522
[34] Lucovsky G, Jing Z, Santos-Fihlo P, Stevens G and Banerjee A 1996 *J. Non-Cryst. Solids* **198–200** 19
[35] Kim Y S and Chang K J 2001 *Phys. Rev. Lett.* **86** 1773
[36] Su T, Taylor P C, Crandall R S and Mahan A H 2000 *Phys. Rev.* B **62** 12849
[37] Chabal Y J and Patel C K N 1984 *Phys. Rev. Lett.* **53** 210
[38] Longeaud C, Roy D and Saadane O 2002 *Phys. Rev.* B **65** 085206
[39] Su T, Taylor P C, Ganguly G and Carlson D E 2002 *Phys. Rev. Lett.* **89** 15502
[40] Meaudre R, Meaudre M, Butté R and Vignoli S 2000 *Thin Solid Films* **366** 207
[41] Beyer W and Abo Ghazala M 1998 *Mater. Res. Soc. Symp. Proc.* **507** 601
[42] Treacy M M J, Gibson J M and Keblinski P J 1998 *J. Non-Cryst. Solids* **231** 99
[43] Voyles P M, Treacy M M J, Jin H-C, Abelson J R, Gibson J M, Yang J, Guha S and Crandall R S 2000 *Mater. Res. Soc. Symp. Proc.* **609** A2.4.1
[44] Voyles P M, Gerbi J E, Treacy M M J, Gibson J M and Abelson J R 2001 *Phys. Rev. Lett.* **86** 5514
[45] Veprek S, Iqbal Z and Sarott F A 1982 *Phil. Mag.* B **45** 137
[46] Kim H Y, Lee K Y and Lee J Y 1997 *Thin Solid Films* **302** 17
[47] Spanakis E, Stratakis E and Tzanetakis P 2001 *J. Appl. Phys.* **89** 4294
[48] Spanakis E, Stratakis E, Tzanetakis P, Fritzsche H, Guha S and Jang J 2002 *J. Non-Cryst. Solids* **299–302** 521
[49] Danesh P and Pantchev B 2000 *Semicond. Sci. Technol.* **15** 971
[50] Boyce J B and Stutzmann M 1985 *Phys. Rev. Lett.* **54** 562
[51] Graebner J E, Golding B, Allen L C, Biegelsen D K and Stutzmann M 1984 *Phys. Rev. Lett.* **52** 553
[52] Jackson W B, Tsai C C and Doland C 1991 *Phil. Mag.* B **64** 611

[53] Fujiwara H, Kondo M and Matsuda A 2001 *Mater. Res. Soc. Symp. Proc.* **664** A1.2.1
[54] Fontcuberta i Morral A and Roca i Cabarrocas P 2001 *Thin Solid Films* **383** 161
[55] Paillard V, Puech P, Sirvin R, Hamma S and Roca i Cabarrocas P 2001 *J. Appl. Phys.* **90** 3276
[56] Yin M T and Cohen M L 1982 *Phys. Rev.* B **26** 5668
[57] Bernstein N, Aziz M J and Kaxiras E 1998 *Phys. Rev.* B **58** 4579
[58] Powell M J, Deane S C and Wehrspohn R B 2002 *Mater. Res. Soc. Symp. Proc.* **715** A11.1
[59] Leopold D J, Fedders P A and Norberg R E 2002 *Mater. Res. Soc. Symp. Proc.* **715** A.1.1
[60] Wehrspohn R B, Deane S C, French I D, Gale I, Hewett J, Powell M J and Robertson J 2000 *J. Appl. Phys.* **87** 144
[61] Gibson J M, Treacy M M J, Voyles P M, Jin H-C and Abelson J R 1998 *Appl. Phys. Lett.* **73** 3093
[62] Baugh J and Han D 2002 *Phys. Rev.* B **66** 115203
[63] Vignoli S, Meaudre R and Meaudre M 1994 *Phys. Rev.* B **50** 7378
[64] Estreicher S K, Hastings J L and Fedders P A 1998 *Phys. Rev.* B **57** R12663
[65] Shimizu T, Maehara T, Mitani M and Kumeda M 2001 *Japan. J. Appl. Phys.* **40** 1244
[66] Roy D, Longeaud C, Saadane O, Gueunier M E, Vignoli S, Butté R, Meaudre R and Meaudre M 2002 *J. Non-Cryst. Solids* **299–302** 482
[67] Fedders P A, Drabold D A and Nakhmanson S 1998 *Phys. Rev.* B **58** 15624
[68] Gotoh T, Nonomura S, Nishio M, Nitta S, Kondo M and Matsuda A 1998 *Appl. Phys. Lett.* **72** 2978
[69] Meaudre M and Meaudre R 2001 *J. Phys.: Condens. Matter* **13** 5663
[70] Kounavis P and Mytilineou E 1995 *Solid State Phenom.* **44–46** 715
[71] Branz H M and Silver M 1990 *Phys. Rev.* B **42** 7420
[72] Koval R, Niu X, Pearce J, Jiao L, Ganguly G, Yang J, Guha S, Collins R W and Wronski C R 2000 *Mater. Res. Soc. Symp. Proc.* **609** A15.5
[73] Meaudre R, Meaudre M, Butté R and Vignoli S 1999 *Phil. Mag. Lett.* **79** 763